

Large Orbital Moments and Internal Magnetic Fields in Lithium Nitridoferrate(I)

J. Klatyk,^{1,*} W. Schnelle,^{1,†} F. R. Wagner,¹ R. Niewa,¹ P. Novák,^{1,‡} R. Kniep,¹ M. Waldeck,²
V. Ksenofontov,² and P. Gütlich²

¹Max-Planck-Institut für Chemische Physik fester Stoffe, Nöthnitzer Straße 40, 01187 Dresden, Germany

²Institut für Anorganische Chemie und Analytische Chemie, Johannes Gutenberg-Universität Mainz, Staudinger-Weg 9,
55099 Mainz, Germany

(Received 24 October 2001; published 1 May 2002)

The iron nitridometalates $\text{Li}_2[(\text{Li}_{1-x}\text{Fe}_x^I)\text{N}]$ display ferromagnetic ordering and spin freezing. Large magnetic moments up to $5.0\mu_B/\text{Fe}$ are found in the magnetization. In Mössbauer effect studies huge hyperfine magnetic fields up to 696 kOe are observed at specific Fe sites. These extraordinary fields and moments originate in an unusual ligand field splitting for those Fe species leading [within local spin density approximation (LSDA)] to a localized orbitally degenerate doublet. Including spin-orbit interaction and strong intra-atomic electron correlation (LDA + SO + U) gives rise to a large orbital momentum.

DOI: 10.1103/PhysRevLett.88.207202

PACS numbers: 75.50.Cc, 71.15.Mb, 75.50.Lk, 76.80.+y

The magnetic behavior of $3d$ -metal compounds is in most cases determined by the spin component of the open d -electron shell. Only for a few ions such as Co^{II} larger orbital contributions to the magnetic moment are observed, which is well understood within ligand field theory. In some diluted systems, however, giant magnetic moments far above the spin-only values are found. Particularly interesting are Fe, Co, or Ni in alkali metal matrices [1,2]. Here, due to extremely weak crystal field (CF) interactions between $3d$ metal and host, the $3d$ angular momentum is no longer quenched and full LS coupling occurs.

Recently, we have synthesized new Fe and Mn nitridometalates [3] with the transition metals T in the unusually low oxidation state +1. The chemical and magnetic properties of the nitridometalate substitution series $\text{Li}_2[(\text{Li}_{1-x}\text{T}_x)\text{N}]$ ($T = \text{Mn}, \text{Fe}, \text{Co}, \text{Ni}, \text{Cu}$) [4,5] turned out to be very unusual. For the Mn, Fe, Co, and Ni compounds the +1 oxidation state of the $3d$ ion could recently be confirmed by x-ray absorption spectroscopy [5].

In this Letter we show that in $\text{Li}_2[(\text{Li}_{1-x}\text{Fe}_x)\text{N}]$ a ferromagnetically ordered state exists, which has magnetic moments greatly exceeding the spin-only value. Comparing to the above mentioned $3d$ impurity systems a large orbital contribution is rather unexpected as the Fe ions are subject to a strong CF. The Fe concentration is high ($x = 0.16$ and $x = 0.21$) and magnetic interactions of order 100 K are present. Moreover, in Mössbauer spectroscopy measurements we observe hyperfine magnetic fields at three iron sites which well exceed that in all other investigated Fe compounds. On the basis of full potential linearized augmented plane wave (FP-LAPW) calculations [6] with inclusion of spin-orbit (SO) coupling and strong intra-atomic correlation [local density approximation (LDA) + U], we trace back the huge hyperfine fields to (i) an energetic sequence of the Fe d -orbitals different than expected from standard ligand field arguments [7] and (ii) the occurrence of a highly localized Fe d -orbital doublet. This state causes

strong orbital contributions to the magnetic moments and the hyperfine fields upon switching on a small SO interaction. The effect is further enhanced by inclusion of strong electronic correlation within LDA + U .

Samples of $\text{Li}_2[(\text{Li}_{1-x}\text{Fe}_x)\text{N}]$ were obtained by decomposition of $\text{Li}_3[\text{Fe}^{\text{III}}\text{N}_2]$ in the presence of Li (molar ratio 1:1) under Ar in an Fe crucible at maximum temperatures of 800 °C for 2 min [3]. Powder x-ray diffraction (XRD) reveals the $\text{Li}_2[(\text{Li}_{1-x}\text{Fe}_x)\text{N}]$ phase and elemental Fe. The substitution parameters $x = 0.21$ and $x = 0.16$ were determined by linear interpolation of the hexagonal lattice parameters [$x = 0.21$: $a = 367.5(4)$ pm, $c = 380.5(4)$ pm [3]]. After grinding and purification from elemental Fe by gradual magnetic separation the final composition of the $x = 0.21$ sample was confirmed by chemical analysis ($x = 0.22$). The $x = 0.16$ sample was synthesized similarly at $T_{\text{max}} = 700$ °C and a longer reaction time (40 h).

$\text{Li}_2[(\text{Li}_{1-x}\text{Fe}_x)\text{N}]$, like the analogous systems with Mn, Co, Ni, and Cu, crystallizes in the $\text{Li}_2[\text{LiN}]$ ($= \alpha\text{-Li}_3\text{N}$) structure type [8] (Fig. 1). Li is partially substituted by Fe only within linear chains $\frac{1}{2}[(\text{Li}_{1-x}\text{Fe}_x^I)\text{N}]$. Because of the random substitution the iron species can have different lateral surroundings of six Li or Fe atoms. Nitrogen is surrounded by six further lithium atoms forming Li_2N layers perpendicular to the $[(\text{Li},\text{Fe})\text{N}]$ chains.

The magnetization of powder samples was measured in a SQUID magnetometer. Field cooling (fc) and zero field cooling on rewarming (zfc) measurements were performed. The corrected high-field susceptibility $1/\chi(T)$ above 200 K can be fitted by a Curie-Weiss law $\chi(T) = C/(T - \theta)$ with $\theta = +76$ K (+136 K) and C corresponding to $\mu_{\text{eff}} = (4.4 \pm 0.3)\mu_B/\text{Fe}$ atom [(5.8 \pm 0.3) μ_B/Fe atom] for the $x = 0.21$ ($x = 0.16$) sample. Thus, in both samples $\mu_{\text{eff}}/\text{Fe}$ atom strongly exceeds the spin-only value for a Fe^{I} high-spin d^7 ion ($3.87\mu_B$). For the d^7 state of Co^{II} 4.30–5.20 μ_B are observed [9]. The positive θ points at a ferromagnetic (fm) exchange interaction, but θ and the $\mu_{\text{eff}}/\text{Fe}$ atom are

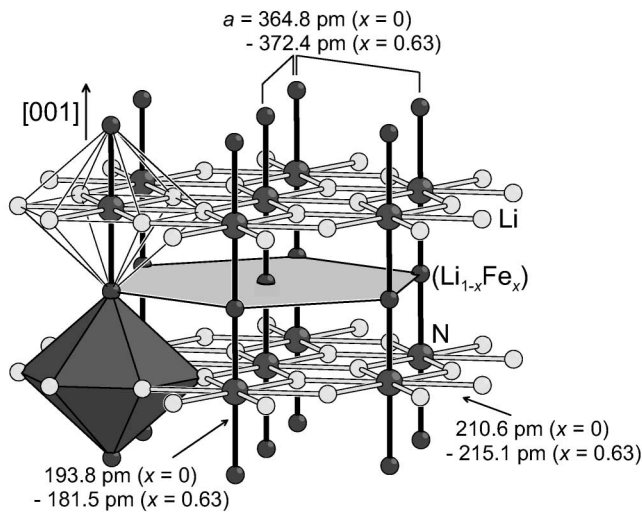


FIG. 1. Part of the crystal structure of $\text{Li}_2[(\text{Li}_{1-x}\text{Fe}_x)\text{N}]$.

larger for the sample with the lower x . Below 200 K a deviation of $1/\chi(T)$ below the Curie-Weiss extrapolation hints to a frustration of the magnetic moments. In Fig. 2 the magnetizations $M(T, H)$ are plotted. In all fc curves a broad increase and a tendency to saturation of $M(T)$ with decreasing T is observed. The temperature of this rise in $M(T)$ increases with H . For $x = 0.21$ at 2 K, M increases slowly with H and reaches $(2.0 \pm 0.3)\mu_B/\text{Fe}$ atom in 70 kOe field, while for $x = 0.16$ and $H \geq 1$ kOe saturation of $M(T)$ around $(5.0 \pm 0.3)\mu_B/\text{Fe}$ atom is observed, i.e., a value much higher than the spin-only $M_{\text{sat}} = 3\mu_B$ expected for a $S = 3/2$ Fe^I ion. The rise in $M(T)$ for low fields occurs at ≈ 60 K (≈ 80 K) in the $x = 0.21$ ($x = 0.16$) sample. The curves $M_{\text{zfc}}(T)$ all start with lower values than the fc data, increase with T to display a maximum (at T_{max}), and then smoothly join M_{fc} . T_{max} increases with decreasing field.

The smooth rise of $M(T, H)$ indicates the gradual fm ordering of the Fe^I moments which is stabilized by exter-

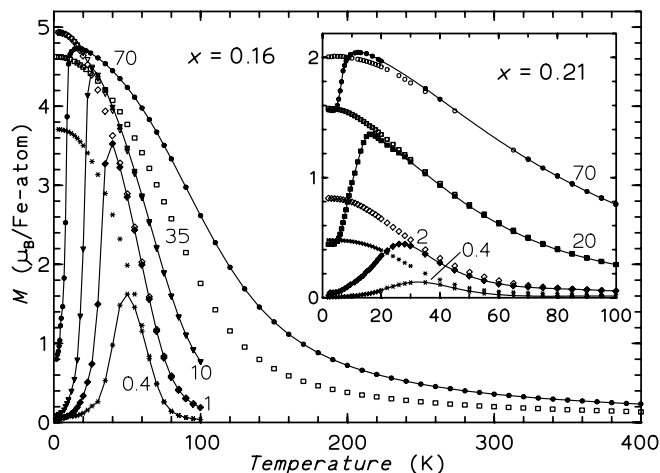


FIG. 2. Temperature dependence of the magnetization of $\text{Li}_2[(\text{Li}_{1-x}\text{Fe}_x)\text{N}]$ ($x = 0.21, 0.16$) measured in zfc (full symbols and lines) and fc (open symbols) modes for external magnetic fields (H/kOe) as indicated by the numbers.

nal fields. At the current stage of experiments the thermal remagnetization, which is characteristic for strong anisotropic magnets with fm domains, is the easiest explanation for the spin freezing. There are some indications for a reentrant-spin-glass (RSG) transition of the $x = 0.16$ sample. This state might exist due to the *random* distribution of the Fe over the hexagonal plane. Also, a RSG is destabilized with field. In ac-susceptibility data [5] ($H_{\text{ac}} = 10$ Oe) a decrease of $\chi_{\text{ac}}(T)$ measured in cooling below T_{max} and the small coercivity at 2 K corroborate the RSG interpretation for $x = 0.16$.

The analysis of the Mössbauer spectra ($x = 0.21$; $4.2 < T < 295$ K) reveals the appearance of fm ordering at $T_C \approx 65$ K. At 295 K, all iron sites give rise to quadrupole doublets with indistinguishable Mössbauer parameters: isomer shift $\delta = -0.026(4)$ mm/s (hereafter with respect to $\alpha\text{-Fe}$) and quadrupole splitting $|\Delta E_Q| = 2.61$ mm/s. Typical relaxation asymmetry is observed in the paramagnetic region and is very pronounced even at 295 K. The 4.2 K Mössbauer spectrum (Fig. 3) exhibits three well-defined groups (A, B, C) of sextets with the parameters A: $H = 696(3)$ kOe, $\delta = +0.121(3)$ mm/s, $\Delta E_Q = -2.61(1)$ mm/s; B: $H = 656(4)$ kOe, $\delta = +0.133(4)$ mm/s, $\Delta E_Q = -2.56(1)$ mm/s; C: $H = 591(15)$ kOe, $\delta = +0.170(4)$ mm/s, $\Delta E_Q = -2.60(1)$ mm/s which can be correlated with three positions with distinct atomic surroundings. Most remarkable are the local magnetic fields. 696 kOe for the main component A and 656 kOe for species B are well above the record values of 624 kOe in $\alpha\text{-Fe}(\text{OETAP})$ [10] and 615 kOe in FeF_3 [11]. Well-defined “static” Mössbauer subspectra with relaxation broadened lines coexist at low temperatures. Their common relative intensity is $\approx 25\%$ and this is too big to be attributed to an impurity in the single-phase sample. Almost identical hyperfine fields are found for $x = 0.16$.

The linewidths of the Mössbauer resonance signals correlate with the structure of the local surroundings. The

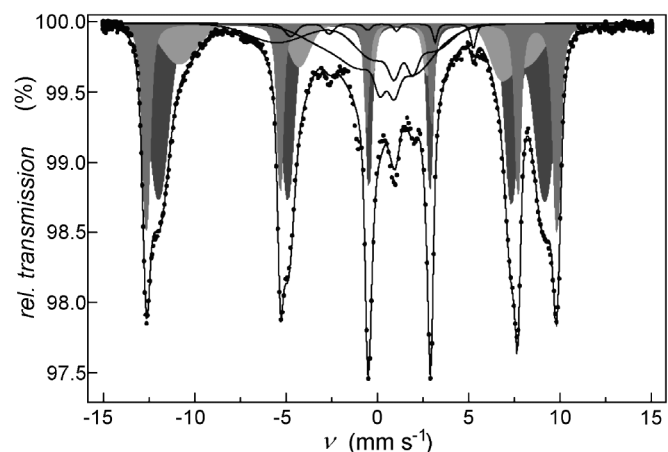


FIG. 3. Mössbauer spectrum of $\text{Li}_2[(\text{Li}_{1-x}\text{Fe}_x)\text{N}]$ recorded at 4.2 K with subspectra (middle grey: species A ($n = 6$), dark: species B ($n = 5$), light: species C ($n = 4$), lines: species D, E, F with $n = 3, 2, 1$, respectively, and fitted sum curve).

narrow lines of the sextet spectrum with the highest value of the magnetic field may be explained by uniform surroundings of the iron species, i.e., Fe with only Li ions as nearest neighbors within the (001) plane (see Fig. 1).

With increasing iron content in the local surroundings of the iron position, different nonequivalent configurations arise leading to an increase of the linewidths. In the structure of the peripheral lines of the Mössbauer spectra one can clearly recognize three Fe sites for which a monotonic increase of linewidths with a concomitant decrease of the hyperfine field is observed. These partial subspectra with hyperfine fields (linewidth, relative area) 696(3) kOe (8.5 kOe, 19.8%), 656(4) kOe (29 kOe, 37.8%), and 591(15) kOe (54 kOe, 15.0%) are attributed to iron centers with lateral surroundings consisting of six Li ($n = 6$, species A), five Li and one Fe ($n = 5$, species B), four Li and two Fe [$n = 4$, species C, $d(\text{Fe}-(\text{Li}, \text{Fe})) = 367.5(4)$ pm]. Two nitrogen ligands in apical positions close the first coordination sphere. Iron-rich environments ($n = 3, 2, 1, 0$) provide the essential part in the middle of the spectrum, which has a relaxation nature even at 4.2 K. A combinatorial analysis has been performed using the expression for the probability to find n Li among six neighbors within the (001) plane: $W_n = 6!/[n!(6-n)!]^{-1}(1-x)^n x^{6-n}$. The value of the iron concentration of $x = 0.25$ from minimization of the functional $F(x) = [(1-x)^6 - 0.198]^2 + [6x(1-x)^5 - 0.378]^2 + [15x^2(1-x)^4 - 0.15]^2 + [20x^3(1-x) + 15x^4(1-x)^2 + 6x^5(1-x) - 0.274]^2$ is in good agreement with those obtained by XRD and chemical analysis. The combinatorial analysis proves that Fe substitutes Li statistically in the $x = 0.21$ sample and supports the proposed site assignment. The $x = 0.16$ sample (prepared at lower temperature) exhibits a significant preference for the $n = 5$ configuration (relative area 46.3%; 18.4% for $n = 6$; 19.1% for $n = 4$).

To understand the magnetism in $\text{Li}_2[(\text{Li}_{1-x}\text{Fe}_x)\text{N}]$ its electronic structure was calculated using the FP-LAPW method [6]. The key ingredient of our Hamiltonian was the spin-orbit (SO) coupling and the inclusion of strong Coulomb correlation for Fe-3d states as approximated by the LDA + U method [12]. The random distribution of Fe was modeled using the supercell approach. Here we consider an especially illustrative model, which contains two different Fe species in a $\sqrt{3} \times \sqrt{3} \times 2$ hexagonal unit cell. The “Fe1” atom possesses six Li as nearest neighbors within the (001) plane (corresponding to species A) while the two “Fe2” atoms have three Li and three Fe neighbors (species D), for which small orbital effects are observed.

The axial CF splits the five 3d orbital states of iron into a doublet $D1$ [states (d_{xz}, d_{yz}) , or equivalently $|M_L = 1\rangle$, $|-1\rangle$], a doublet $D2$ [states $(d_{xy}, d_{x^2-y^2})$, or $|2\rangle$, $|-2\rangle$], and a singlet S (d_{z^2} , or $|0\rangle$). For the expected $3d^7$ configuration and in the weak CF scheme the majority spin electrons occupy all five orbital states, while the distribution of the minority spin electrons depends on the energy sequence of $D1$, $D2$, and S . A simple ligand field picture

would predict that, because of the strong $d_{z^2}(\text{Fe})-p_z(\text{N})$ hybridization, the singlet S possesses the highest energy. In such a case the resulting state of Fe^I would be orbitally nondegenerate. Our electronic structure calculations point to a different sequence. All 3d majority spin energy levels lie below the Fermi energy E_F , in accord with the weak CF scheme. However, in contrast to the ligand field prediction, for the minority spins the singlet S has the lowest energy, doublet $D1$ is the highest and it is unoccupied, while the doublet $D2$ is intersected by E_F (Fig. 4). Detailed analysis shows that the unusual energy scheme is a consequence of an on-site, CF induced $3d_{z^2}-4s$ mixing [7]. Because of the lack of bonding partners within the (001) plane the $\text{Fe}1(d_{xy}, d_{x^2-y^2})$ states are strongly localized and their peak in the density of states is narrow (FWHM < 50 meV). Therefore, SO coupling is strong enough to split this peak by decreasing the energy of $M_L = 2$ states, moving them partially below E_F and increasing the energy of $M_L = -2$ states, which become less occupied. As a consequence a large orbital momentum appears.

Using the force theorem [13] and the LSDA method we calculated the magnetocrystalline anisotropy and obtained $E_c - E_a = -10.5(5)$ meV/(unit cell), where E_c and E_a are the total energies for magnetization $\parallel c$ axis and $\parallel a$ axis, respectively. The hexagonal c axis therefore is the easy direction for magnetization and the anisotropy is very large for a 3d metal compound. Therefore, all calculations with SO coupling were performed with $M \parallel c$.

Within LDA + SO the projection of the orbital momentum on the hexagonal axis is $L_c = 0.75$ (see Table I). The orbital momentum obtained so far is further enhanced by

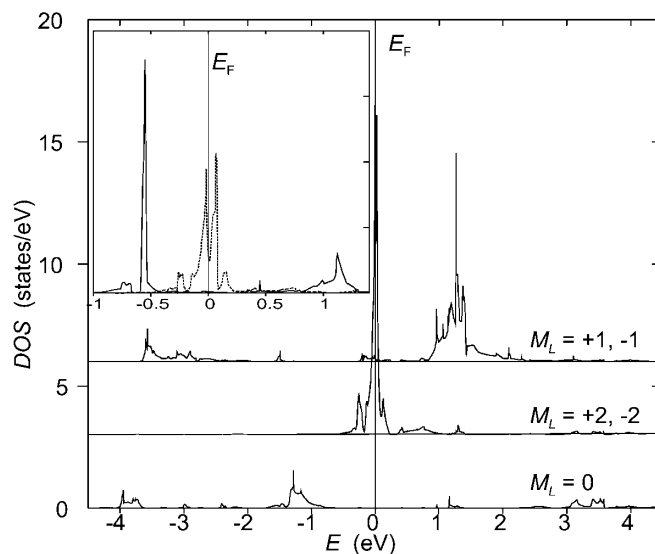


FIG. 4. Scalar relativistic local spin density approximation (LSDA) density of states for the minority spin channel corresponding to $M_L = 0$, $M_L = \pm 2$, and $M_L = \pm 1$ states of the Fe1 ion. Inset: Modification of the $M_L = \pm 2$ density of states by the SO coupling (dashed curve) and by LDA + U combined with SO coupling (full curve, parameters $U = 4$ eV, $J = 0.5$ eV).

TABLE I. Hyperfine fields H (kOe), electric field gradients (EFG) (10^{21} V m $^{-2}$; experimental average value), magnetic orbital and spin moments, μ_L and μ_S (μ_B), for two inequivalent Fe ions, calculated using LDA + SO and LDA + SO + U methods. The values of U and J were 4 and 0.5 eV (LDA + SO + U_1) and 8 and 1 eV (LDA + SO + U_2). Experimental values are for $x = 0.21$.

Site		LDA + SO	+ U_1	+ U_2	Expt.
Fe1 (A) $n = 6$	H_{cont}	-60	-83	-102	
	H_{orb}	524	955	1015	
	H_{dip}	17	-10	-34	
	H_{tot}	481	862	879	694(3)
	EFG	-16.8	-14.0	-11.4	≈ -18
	μ_L	0.75	1.37	1.45	
	μ_S	2.39	2.59	2.74	
Fe2 (B) $n = 3$	H_{cont}	61	-40	-135	
	H_{orb}	182	98	36	
	H_{dip}	12	30	72	
	H_{tot}	255	88	-27	$\approx 170(50)$
	EFG	-16.7	-19.3	-24.7	≈ -18
	μ_L	0.26	0.14	0.06	
	μ_S	2.50	2.88	3.21	

the LDA + U , because the energy of states with larger (smaller) occupation is decreased (increased). The splitting of the $D2$ peak by SO coupling and by electron correlation, as obtained using LDA + U , is shown in the inset of Fig. 4. This figure suggests that the resulting value of L_c would be almost independent of the values of U and J , providing these are kept within reasonable limits. Indeed, increasing the value of U from 4 to 8 eV resulted in a change of L_c from 1.37 to $1.45\mu_B$ (see Table I).

The Fe2($d_{xy}, d_{x^2-y^2}$) states also lie at E_F , but due to Fe-Fe hybridization, the corresponding bands are broader. As a consequence, SO coupling and LDA + U produce much smaller orbital moments ($0.06-0.26\mu_B$).

The hyperfine field H_{hf} on the Fe nuclei may be written as $H_{\text{hf}} = H_{\text{cont}} + H_{\text{orb}} + H_{\text{dip}} + H_{\text{latt}}$, where H_{cont} is the Fermi contact term, H_{orb} and H_{dip} are contributions from the “on-site” interaction of the nuclear magnetic momentum with the electronic orbital and the spin momentum, respectively. H_{latt} corresponds to the interaction with other electronic magnetic moments and was neglected here. For the calculation of H_{orb} and H_{dip} , the method of Blügel *et al.* [14] was employed. The results are summarized in Table I: H_{cont} is always smaller than H_{orb} . The field on Fe1 nuclei comes out larger in LDA + U than observed. This is not surprising, because (i) the contact field on iron nuclei is underestimated in the DFT calculations [15] and as H_{cont} and H_{orb} have opposite signs, this will decrease the total field and (ii) more important, random strains will cause broadening of the $|\pm 2\rangle$ peak in the density of states (Fig. 4). As a consequence smaller L_c would be obtained in LDA + SO and LDA + SO + U calculations, leading to a smaller H_{orb} .

Summarizing, we observe a peculiar new feature for a $3d$ metal compound: it is generally accepted that CF quenches a part or all of the orbital momentum of a free $3d$ ion. For cubic symmetry a maximum of $L = 1$ is possible and reduction of symmetry leads to further quenching of L . For the compound studied, we showed that due to the special electronic circumstances orbital moments of up to $L = 2$ may be observed in an axial CF. In conclusion, the huge hyperfine magnetic fields and the large magnetic moments found in the fm ordered phase $\text{Li}_2[(\text{Li}_{1-x}\text{Fe}_x^{\text{I}})\text{N}]$ can be explained by these strong orbital contributions within a relativistic LDA + U scheme.

We thank the DFG and the Fonds der Chemischen Industrie for financial support.

*Now at Merck KGaA, Darmstadt, Germany.

†Electronic address: schnelle@cpfs.mpg.de

‡Permanent address: Institute of Physics, ASCR, Cukrovarnická 10, 16253 Praha 6, Czech Republic.

- [1] D. Riegel *et al.*, Phys. Rev. Lett. **57**, 388 (1986); R. Kowalik *et al.*, *ibid.* **63**, 434 (1989).
- [2] H. Beckmann and G. Bergmann, Phys. Rev. Lett. **83**, 2417 (1999); **85**, 1584 (2000); M. Gruyters and D. Riegel, *ibid.* **85**, 1582 (2000); P. Mohn *et al.*, *ibid.* **85**, 1583 (2000); S. K. Kwon and B. I. Min, *ibid.* **84**, 3970 (2000).
- [3] J. Klatyk and R. Kniep, Z. Kristallogr. New Cryst. Struct. **214**, 445 (1999); **214**, 447 (1999); J. Klatyk, Ph.D. thesis, Technische Universität Darmstadt, 1999.
- [4] W. Sachsze and R. Juza, Z. Anorg. Allg. Chem. **259**, 278 (1949); R. Kniep, Pure Appl. Chem. **69**, 185 (1997).
- [5] R. Niewa *et al.* (unpublished).
- [6] P. Blaha, K. Schwarz, and J. Luitz, WIEN97, *A Full Potential Linearized Plane Wave Package for Calculating Crystal Properties* (K. Schwarz, Wien, Austria, 1999), ISBN 3-9501031-0-4.
- [7] For linear transition metal dichloride molecules a similar effect has been discussed recently. S. G. Wang and W. H. E. Schwarz, J. Chem. Phys. **109**, 7252 (1998).
- [8] A. Rabenau and H. Schulz, J. Less-Common Met. **50**, 155 (1976).
- [9] E. König and G. König, in *Landolt-Börnstein, Neue Serie*, edited by K.-H. Hellwege (Springer-Verlag, Berlin, 1984), Vol. 12.
- [10] W. M. Reiff, C. M. Frommen, G. T. Yee, and S. P. Sellers, Inorg. Chem. **39**, 2076 (2000).
- [11] G. K. Wertheim, H. J. Guggenheim, and D. N. E. Buchanan, Phys. Rev. **169**, 465 (1968).
- [12] A. I. Liechtenstein, V. I. Anisimov, and J. Zaanen, Phys. Rev. B **52**, R5467 (1995).
- [13] A. R. Mackintosh and O. K. Andersen, in *Electrons at the Fermi Surface*, edited by M. Springford (Cambridge University Press, Cambridge, 1980), pp. 149–224.
- [14] S. Blügel, H. Akai, R. Zeller, and P. H. Dederichs, Phys. Rev. B **35**, 3271 (1987).
- [15] R. Coehoorn, J. Magn. Magn. Mater. **159**, 55 (1996).